AIMS Mathematics, 11(4): 11580–11594.
DOI: 10.3934/math.2026477
Received: 20 February 2026
Revised: 13 April 2026
Accepted: 21 April 2026
Published: 27 April 2026

http://www.aimspress.com/journal/Math

Research article

Higher-order smooth profiles and breather-positon phenomena in the Kuralay equation

Maha Alammari[1], Muhammad Yasir[2] and Solomon Manukure[3,*]

[1] Department of Mathematics, College of Science, King Saud University, P.O. Box 22452 Riyadh 11495, Saudi Arabia
[2] School of Mathematics, Hefei University of Technology, Hefei 230009, China
[3] Florida A & M University, Tallahassee, FL, 3230, USA

* **Correspondence:** Email: solomon.manukure@famu.edu.

Abstract: In this paper, we investigated higher-order smooth positon and breather-positon solutions of the Kuralay equation. Starting from the associated Lax pair, we constructed an explicit N-fold Darboux transformation (DT) in determinant form. By introducing a spectral parameter degeneration procedure combined with higher-order Taylor expansion, we derived smooth higher-order positon solutions from multi-soliton solutions. Furthermore, under nonvanishing boundary conditions, breather-positon solutions were obtained. The dynamical properties of these solutions were analyzed, revealing elastic interaction behavior and nontrivial phase shifts. The results provided a unified framework for constructing degenerate localized wave structures and extended existing studies on the Kuralay equation.

Keywords: degenerate Darboux transformation; Positon solutions; phase Shifts; breather-positon
Mathematics Subject Classification: 35J05, 35K05, 35L05, 37K40

1. Introduction

Integrable systems constitute a distinguished class of nonlinear partial differential equations that possess rich mathematical structures and admit exact analytical solutions [1–4]. The solvability of such systems is typically ensured by powerful analytical techniques, including the inverse scattering transform [5], the Darboux transformation (DT) [6–8], and Hirota's bilinear method [9, 10]. In recent years, inverse scattering, DT, and spectral analysis methods have continued to develop rapidly, providing deeper insights into the structure of integrable systems and their exact solutions [11, 12]. Besides the DT, other methods such as the Hirota bilinear method and recent neural network-based

approaches [13, 14] have been developed to obtain exact and approximate solutions of nonlinear partial differential equations. Compared with these approaches, the DT provides a direct algebraic framework for constructing exact solutions of integrable systems. These methods enable the systematic construction of exact wave solutions and reveal the deep algebraic and geometric properties underlying nonlinear evolution equations. Among the most remarkable solutions obtained through these approaches are solitons [15, 16]. Solitons represent stable, localized wave structures that emerge from an exact balance between nonlinear effects and dispersive mechanisms [17]. They behave like particle-like entities, maintaining their shape, velocity, and amplitude during propagation and even after nonlinear interactions. Due to these exceptional characteristics, solitons occupy a central position in nonlinear science and have been widely investigated in various physical settings, including nonlinear optics, plasma physics, fluid dynamics, and ferromagnetic systems [18].

Beyond classical solitons, integrable systems admit a variety of other localized wave structures with richer dynamical behaviors. Among them, breathers represent an important class of nonlinear excitations characterized by periodic oscillations in amplitude or width during propagation [19, 20]. Depending on their localization properties, breathers are commonly classified into Akhmediev breathers [21], which are periodic in space and localized in time, Kuznetsov–Ma breathers [22], which are periodic in time and localized in space, and more general breather solutions. Breathers play a crucial role in the description of modulation instability and are closely related to the formation of rogue waves through suitable limiting processes [23]. Soliton and related localized wave structures play an important role in various physical systems. For example, the collapse of soliton-like cavitation bubbles in fluids can generate highly localized energy release, which has recently been utilized for micro-scale propulsion and manipulation [24]. In addition, optical solitons are fundamental in fiber laser systems and nonlinear optical communication, where they enable stable pulse propagation over long distances [25]. These developments highlight the practical significance of studying nonlinear localized wave structures in integrable systems.

Another intriguing class of solutions in integrable systems is the so-called positon. Positons can be viewed as degenerate limits of multi-soliton solutions when distinct spectral parameters coalesce [26]. Unlike solitons, which are expressed purely in terms of exponential functions, positon solutions typically involve a mixture of exponential and polynomial terms, leading to slower spatial decay and long-range oscillatory structures [27]. Despite their nonstandard asymptotic behavior, positons remain smooth and nonsingular, and their interaction properties exhibit features fundamentally different from those of classical solitons.

More recently, breather-positon solutions have attracted increasing attention. These solutions arise from the degeneration of breather solutions and combine the oscillatory nature of breathers with the algebraic features of positons [28]. As a result, breather-positons exhibit hybrid dynamical characteristics, including localized oscillations accompanied by slowly varying envelopes. The study of breather-positons provides deeper insight into the internal structure of nonlinear waves and the role of spectral degeneracy in integrable systems [29]. Therefore, it is of interest to develop a unified framework for constructing higher-order smooth positon and breather-positon solutions of the Kuralay equation.

In this paper, we consider the Kuralay equation [20, 30, 31]

$$\begin{aligned} \mathrm{i}q_t + q_{xx} + vq = 0, \\ v_t + (|q|^2)_x = 0, \end{aligned} \tag{1.1}$$

which is an integrable system admitting a Lax pair representation and arising in nonlinear wave theory and geometric curve flow models. The Kuralay equation admits both physical and geometrical interpretations. From the viewpoint of nonlinear wave theory, the complex function $q(x,t)$ represents a wave envelope, while $v(x,t)$ is a real-valued potential describing a self-consistent field. The term $\mathrm{i}q_t$ corresponds to temporal evolution, the dispersive term governs wave spreading, and the coupling term vq represents nonlinear interaction between the wave and the background field. On the other hand, the Kuralay equation admits a geometrical interpretation as the integrable motion of space curves in $\mathbb{R}^3$, as established in [31]. In particular, it is gauge equivalent to a Heisenberg-type spin system, where the dynamics are described by a unit spin vector $\mathbf{S}(x,t)$. In this representation, the complex field q and the potential v are related to geometric quantities such as curvature and torsion of the evolving curve. These solutions provide insight into nonlinear wave phenomena observed in physical systems such as optical fibers, fluid waves, and plasma dynamics.

Although soliton, breather, and rogue-wave solutions of this system have been extensively studied [7, 20, 32, 33], the systematic construction of higher-order smooth positon and breather-positon solutions via spectral degeneration remains limited, which motivates the present study. The Kuralay equation has been widely studied in recent years due to its rich integrable structure and diverse applications. Various analytical and numerical approaches have been developed to investigate its soliton dynamics, exact solutions, and physical properties [34–36]. In particular, the role of spectral parameter degeneration in generating such higher-order structures has not been systematically explored. In this work, we construct higher-order smooth positon and breather-positon solutions by means of a direct N-fold DT. Starting from the associated Lax pair, we establish an explicit transformation formula and implement a suitable degeneration procedure to obtain higher-order solutions in a unified framework. The interaction characteristics of the resulting solutions are further examined.

It should be emphasized that the DT used in this paper follows the standard determinant representation associated with the Lax pair of the Kuralay equation. The novelty of the present work does not lie in introducing a new elementary DT, but in the systematic implementation of a degenerate N-fold DT combined with higher-order Taylor expansion. This enables the explicit construction of higher-order smooth positon solutions from the coalescence of soliton spectral parameters, and further yields breather-positon solutions under nonvanishing boundary conditions within a unified framework. Within this framework, positon and breather-positon solutions can be interpreted as special nonlinear wave patterns generated by spectral degeneracy, exhibiting long-range oscillatory behavior and nontrivial modulation on zero or nonzero backgrounds.

The remainder of this paper is organized as follows. In Section 2, we present the Lax pair formulation and derive the direct N-fold DT. In Section 3, we construct higher-order positon and breather-positon solutions and analyze their dynamical properties. Finally, Section 4 concludes the paper.

2. Lax pair and the direct N-fold DT

The DT provides an effective algebraic procedure for constructing new solutions of integrable equations from known ones. The essential idea is to transform a given Lax pair into another Lax pair of identical structure, thus establishing a direct link between seed solutions and their transformed

counterparts. For System (1.1), a Lax representation was presented in [33] in the form

$$\begin{aligned} &\psi_x = U\psi, \quad \psi_t = V\psi, \\ &U = \mathrm{i}\lambda\sigma_3 + Q, \quad V = 2\mathrm{i}\lambda^2\sigma_3 + 2\lambda Q + \mathrm{i}v\sigma_3 + Q_x. \end{aligned} \tag{2.1}$$

Here,

$$\sigma_3 = \begin{pmatrix} 1 & 0 \\ 0 & -1 \end{pmatrix}, \qquad Q = \begin{pmatrix} 0 & q \\ -q^* & 0 \end{pmatrix},$$

$\mathrm{i} = \sqrt{-1}$, and λ denotes a complex spectral parameter. The vector function $\psi = (\psi_1 \quad \psi_2)^T$ represents the eigenfunction associated with the spectral problem, where ψ_1 and ψ_2 are complex-valued functions depending on x and t, and T stands for matrix transposition. The zero-curvature condition $\psi_{xt} = \psi_{tx}$ corresponding to (2.1) recovers System (1.1).

For the construction of the N-fold DT, we introduce $2N$ eigenfunctions of the Lax pair (2.1),

$$\psi_{2j-1} = \psi(\lambda)\big|_{\lambda=\lambda_{2j-1}} = \begin{pmatrix} \psi_{2j-1,1} \\ \psi_{2j-1,2} \end{pmatrix}, \quad \psi_{2j} = \psi(\lambda)\big|_{\lambda=\lambda_{2j}} = \begin{pmatrix} \psi_{2j,1} \\ \psi_{2j,2} \end{pmatrix}, \tag{2.2}$$

for $j = 1, 2, \ldots, N$. These eigenfunctions are required to satisfy the reduction condition

$$\lambda_{2j} = \lambda_{2j-1}^*, \qquad \psi_{2j} = \begin{pmatrix} -\psi_{2j-1,2}^* \\ \psi_{2j-1,1}^* \end{pmatrix}, \tag{2.3}$$

which guarantees that the transformed potentials remain real-valued in the appropriate sense.

On the basis of (2.1)–(2.3), both the one-fold and the general N-fold DTs can be formulated, and explicit determinant representations for the resulting exact solutions follow accordingly. Following the approach in [37], we adopt a first-order gauge transformation that converts the Lax pair (2.1) into a new pair of the same type, where the potentials q and v are replaced by their first iterates $q^{[1]}$ and $v^{[1]}$. Here, $q^{[1]}$ and $v^{[1]}$ denote the new potentials generated from the seed solution $(q^{[0]}, v^{[0]})$ by the one-fold DT. Similarly, $q^{[N]}$ and $v^{[N]}$ denote the potentials generated by the N-fold transformation. Specifically,

$$\psi^{[1]} = \widetilde{T}_1(\lambda)\psi, \tag{2.4}$$

with the Darboux matrix given by

$$\widetilde{T}_1(\lambda) = \lambda I + \begin{pmatrix} a_0 & b_0 \\ c_0 & d_0 \end{pmatrix}, \tag{2.5}$$

where I denotes the 2×2 identity matrix. The entries of $\widetilde{T}_1(\lambda)$ are uniquely determined from the kernel relations

$$\widetilde{T}_1(\lambda_k)\psi_k = 0. \tag{2.6}$$

The resulting one-fold DT yields new exact solutions of the Kuralay equation,

$$q^{[1]} = q^{[0]} - 2\mathrm{i}b_0, \quad v^{[1]} = v^{[0]} - 4\mathrm{i}a_{0t}, \tag{2.7}$$

with coefficients

$$a_0 = -\frac{\begin{vmatrix} \lambda_1\psi_{11} & \psi_{12} \\ \lambda_2\psi_{21} & \psi_{22} \end{vmatrix}}{\begin{vmatrix} \psi_{11} & \psi_{12} \\ \psi_{21} & \psi_{22} \end{vmatrix}}, \quad b_0 = -\frac{\begin{vmatrix} \psi_{11} & \lambda_1\psi_{11} \\ \psi_{21} & \lambda_2\psi_{21} \end{vmatrix}}{\begin{vmatrix} \psi_{11} & \psi_{12} \\ \psi_{21} & \psi_{22} \end{vmatrix}}. \tag{2.8}$$

The explicit time-dependent term in $v^{[1]}$ arises from the time part of the Lax pair under the DT. In particular, the compatibility condition introduces contributions involving time derivatives of the transformation coefficients, which lead to the appearance of t-dependent terms in the transformed potential. Substituting the resulting expressions into Eq (1.1) confirms that the transformed solutions satisfy the original system.

The one-fold DT can be extended to an N-fold DT in the polynomial form

$$\widetilde{T_N}(\lambda) = \lambda^N I + \lambda^{N-1} t_{N-1} + \cdots + \lambda t_1 + t_0, \tag{2.9}$$

where the coefficient matrices t_j depend on (x, t). The matrix $\widetilde{T_N}$ is uniquely determined by the kernel conditions

$$\widetilde{T_N}(\lambda_k)\psi_k = 0, \qquad k = 1, 2, \ldots, 2N, \tag{2.10}$$

and admits a determinant representation. The transformed eigenfunctions are given by

$$\psi_j^{[N]} = \widetilde{T_N}(\lambda_j)\psi_j = \frac{1}{|W_N|} \begin{bmatrix} \begin{vmatrix} \widetilde{\psi_{N1}} & \lambda\psi_{j1} \\ W_N & \widetilde{\xi_{2N-1}} \end{vmatrix} \\ \\ \begin{vmatrix} \widetilde{\psi_{N1}} & \lambda\psi_{j2} \\ W_N & \widetilde{\xi_{2N}} \end{vmatrix} \end{bmatrix}, \tag{2.11}$$

where the block determinant W_N is defined by

$$W_N = \begin{bmatrix} \psi_{11} & \psi_{12} & \lambda_1\psi_{11} & \lambda_1\psi_{12} & \cdots & \lambda_1^{N-1}\psi_{11} & \lambda_1^{N-1}\psi_{12} \\ \psi_{21} & \psi_{22} & \lambda_2\psi_{21} & \lambda_2\psi_{22} & \cdots & \lambda_2^{N-1}\psi_{21} & \lambda_2^{N-1}\psi_{22} \\ \psi_{31} & \psi_{32} & \lambda_3\psi_{31} & \lambda_3\psi_{32} & \cdots & \lambda_3^{N-1}\psi_{31} & \lambda_3^{N-1}\psi_{32} \\ \psi_{41} & \psi_{42} & \lambda_4\psi_{41} & \lambda_4\psi_{42} & \cdots & \lambda_4^{N-1}\psi_{41} & \lambda_4^{N-1}\psi_{42} \\ \vdots & \vdots & \vdots & \vdots & \ddots & \vdots & \vdots \\ \psi_{2N-1\,1} & \psi_{2N-1\,2} & \lambda_{2N-1}\psi_{2N-1\,1} & \lambda_{2N-1}\psi_{2N-1\,2} & \cdots & \lambda_{2N-1}^{N-1}\psi_{2N-1\,1} & \lambda_{2N-1}^{N-1}\psi_{2N-1\,2} \\ \psi_{2N\,1} & \psi_{2N\,2} & \lambda_{2N}\psi_{2N\,1} & \lambda_{2N}\psi_{2N\,2} & \cdots & \lambda_{2N}^{N-1}\psi_{2N\,1} & \lambda_{2N}^{N-1}\psi_{2N\,2} \end{bmatrix}. \tag{2.12}$$

The vectors $\widetilde{\psi_{N1}}$, $\widetilde{\xi_{2N-1}}$, and $\widetilde{\xi_{2N}}$ are defined by

$$\begin{aligned} \widetilde{\psi_{N1}} &= (\psi_{11}, \psi_{12}, \lambda_1\psi_{11}, \lambda_1\psi_{12}, \ldots, \lambda_N^{N-1}\psi_{11}, \lambda_1^{N-1}\psi_{12}), \\ \widetilde{\xi_{2N-1}} &= (\lambda_1^N\psi_{11}, \lambda_2^N\psi_{21}, \ldots, \lambda_{2N-1}^N\psi_{2N-1\,1}, \lambda_{2N}^N\psi_{2N\,1})^T, \\ \widetilde{\xi_{2N}} &= (\lambda_1^N\psi_{12}, \lambda_1^N\psi_{22}, \ldots, \lambda_{2N-1}^N\psi_{2N-1\,2}, \lambda_{2N}^N\psi_{2N\,2})^T. \end{aligned} \tag{2.13}$$

It follows directly that $\psi_j^{[N]} = 0$ for $j = 1, 2, \ldots, 2N$, showing that $\widetilde{T_N}(\lambda)$ annihilates the generating eigenfunctions.

Applying $\widetilde{T_N}$ yields the Nth-order solutions

$$q^{[N]} = q^{[0]} - 2\mathrm{i}b_{N-1}, \quad v^{[N]} = v^{[0]} - 4\mathrm{i}a_{N-1t}, \tag{2.14}$$

where

$$a_{N-1} = -\frac{W_{N1}}{|W_N|}, \quad b_{N-1} = -\frac{W_{N2}}{|W_N|}. \tag{2.15}$$

The determinants W_{N1} and W_{N2} are obtained from W_N by replacing its columns as follows: W_{N1} is formed by substituting the second last column of W_N with the vector $\widetilde{\xi_{2N-1}}$, and W_{N2} is formed by replacing the last column of W_N with $\widetilde{\xi_{2N}}$.

The N-fold DT thus provides a direct and systematic construction of higher-order exact solutions of the Kuralay equation.

Taking the seed solutions $q^{[0]} = 0$ and $v^{[0]} = c$, the eigenfunctions corresponding to λ_j are given by

$$\psi_j = \psi(\lambda_j) = \begin{pmatrix} \psi_1(x,t,\lambda_j) \\ \psi_2(x,t,\lambda_j) \end{pmatrix} = \begin{pmatrix} e^{\mathrm{i}\lambda_j x + \frac{\mathrm{i}c}{2(2\lambda_j - 1)}t} \\ e^{-\mathrm{i}\lambda_j x - \frac{\mathrm{i}c}{2(2\lambda_j - 1)}t} \end{pmatrix}. \tag{2.16}$$

For $N = 1$, letting $\lambda_2 = \lambda_1^*$, $\lambda_1 = \xi_1 + \mathrm{i}\sigma_1$ with $\xi_1, \sigma_1 \in \mathbb{R}$, the explicit formulas of one-soliton solutions are as follows:

$$q_{1-s} = -2\sigma_1 e^{\mathrm{i}\left(2\xi_1 x + \frac{(2\xi_1 - 1)ct}{4R}\right)} \operatorname{sech}\left(2\sigma_1 x - \frac{\sigma_1 ct}{2R}\right), \tag{2.17}$$

$$v_{1-s} = c - \frac{2c\sigma_1^2}{R} \operatorname{sech}^2\left(2\sigma_1 x - \frac{\sigma_1 ct}{2R}\right), \tag{2.18}$$

where $R = \sigma_1^2 + \left(\xi_1 - \frac{1}{2}\right)^2$.

Throughout this paper, λ denotes the spectral parameter, $\psi = (\psi_1, \psi_2)^T$ represents the eigenfunction of the Lax pair, while ψ_j denotes the eigenfunction evaluated at the spectral parameter λ_j, and $(\cdot)^*$ denotes complex conjugation.

3. Positons and breather positons of Kuralay equation

The positon and breather-positon solutions obtained in this work represent nonlinear localized wave structures with distinct propagation characteristics. In the context of nonlinear wave theory, the function $q(x,t)$ describes the amplitude of a wave envelope, while $v(x,t)$ represents a self-consistent potential field. Unlike classical soliton solutions, which exhibit localized and exponentially decaying profiles, positon solutions display slowly decaying oscillatory behavior due to the presence of polynomial–exponential terms. This leads to long-range interactions and more complex wave structures. The breather-positon solutions combine oscillatory behavior with algebraic features, representing modulated wave packets on a background field. Such structures can be interpreted as nonlinear wave patterns exhibiting both localization and periodic modulation, which are relevant in physical systems such as nonlinear optics, fluid dynamics, and plasma waves.

In this section, we derive positon and breather-positon solutions of the Kuralay equation through a degeneration procedure applied to the N-fold DT. The degeneration procedure used to construct positon solutions corresponds to the coalescence of spectral parameters in the DT. Specifically, when distinct

spectral parameters approach a common value, the standard multi-soliton solutions degenerate into new structures. This coalescence leads to the appearance of hybrid polynomial–exponential terms in the resulting solutions, which is a characteristic feature of positon-type solutions. As a result, positons exhibit slower decay and more complex spatial structures compared to classical solitons.

3.1. Higher-order positons

If $\lambda_3 = \lambda_1$ and $N = 2$ in Eq (2.14), the denominator of the corresponding two-soliton solution vanishes. To construct degenerate solutions, we consider the coalescence of spectral parameters by introducing a perturbation

$$\lambda_{2j-1} = \lambda_1 + \epsilon, \quad \epsilon \to 0, \quad (j = 2, 3, \ldots, N).$$

In this limit, the determinant expressions associated with the N-fold DT lead to an indeterminate form of type $(\frac{0}{0})$. To resolve this, we expand each entry of the determinant in a Taylor series with respect to ϵ:

$$f(\lambda_1 + \epsilon) = \sum_{k=0}^{\infty} \frac{\epsilon^k}{k!} \frac{\partial^k f}{\partial \lambda^k}\Big|_{\lambda=\lambda_1}.$$

Due to the multilinearity of determinants, this expansion transforms the original determinant into a structure involving derivatives of eigenfunctions. As a result, the degenerate DT yields a Wronskian-type representation.

The derivative order is chosen as

$$n_{i=}\left\lfloor \frac{i+1}{2} \right\rfloor,$$

which guarantees linear independence of rows and ensures a nontrivial limiting solution.

This procedure generates smooth positon solutions as a degenerate limit of multi-soliton solutions without introducing singularities. In this way, smooth positon solutions can be constructed from the zero seed through the degenerate N-fold DT. Substituting ψ_j into the degenerate transformation and introducing the determinant forms W_{N1}, W_{N2}, and W_N as defined below, one obtains the N-positon solution of the Kuralay equation.

Proposition 1. *Let the seed solution be $q^{[0]} = 0$ and $v^{[0]} = c$. In the degenerate limit $\lambda_{2j-1} \to \lambda_1$ of the N-fold DT, the resulting N-soliton solution reduces to an N-positon solution of the Kuralay equation given by*

$$q_{n-p} = 2\mathrm{i}\frac{W'_{N2}}{W'_N}, \quad v_{n-p} = c + 4\mathrm{i}\left(\frac{W'_{N1}}{W'_N}\right)_t, \tag{3.1}$$

where

$$W'_{N1} = \left(\frac{\partial^{n_i-1}}{\partial\epsilon^{n_i-1}}\Big|_{\epsilon=0} (W_{N1})_{ij}\,(\lambda_1+\epsilon)\right)_{2N\times 2N}, \tag{3.2}$$

$$W'_{N2} = \left(\frac{\partial^{n_i-1}}{\partial\epsilon^{n_i-1}}\Big|_{\epsilon=0} (W_{N2})_{ij}\,(\lambda_1+\epsilon)\right)_{2N\times 2N}, \tag{3.3}$$

$$W'_{N} = \left(\frac{\partial^{n_i-1}}{\partial\epsilon^{n_i-1}}\Big|_{\epsilon=0} (W_{N})_{ij}\,(\lambda_1+\epsilon)\right)_{2N\times 2N} \tag{3.4}$$

and

$$n_i = \left\lfloor \frac{i+1}{2} \right\rfloor,$$

where $\lfloor \cdot \rfloor$ *denotes the floor function.*

The reduction conditions corresponding to proposition 1 are

$$\lambda_{2j} = \lambda^{(}_{2j-1}*), \qquad \psi_{2j} = \begin{pmatrix} -\psi^*_{2j-1,2} \\ \psi^*_{2j-1,1} \end{pmatrix}, \qquad j = 1, 2, \ldots, N.$$

For brevity, we restrict ourselves to the explicit two-positon case obtained by setting $N = 2$ in proposition 1, since the general expressions become increasingly lengthy. The explicit formulas for the two-positon solution are presented below.

$$q_{2-p} = \frac{16\left(A_1 \sinh\left(B_2\right) + A_2 \cosh\left(B_2\right)\right)\sigma_1}{2R^2 \cosh\left(\frac{\sigma_1(ct-4Rx)}{R}\right) + 2R^2 + 16\sigma_1^2\Big((ct-4Rx)^2 + c\sigma_1^2 tx\Big)}, \tag{3.5}$$

$$v_{2-p} = c + \frac{16c\sigma_1^2\Big(-RA_3\cosh(B_2) + 2A_5\cosh(\frac{1}{2}B_2) - RA_4\Big)}{\Big(2R^2\cosh(B_2) + 2A_6\cosh(\frac{1}{2}B_2) + 2R^2\Big)^2}. \tag{3.6}$$

$$\begin{aligned}
A_1 =& \sigma_1\left(2xR^2 + \frac{ct}{2}\left(2\sigma_1^2 - R\right)\right), \quad A_2 = -R^2 + \mathrm{i}ct\left(\xi_1 - \tfrac{1}{2}\right)\sigma_1^2,\\
B_1 =& \frac{\mathrm{i}\Big(8\xi_1 xR + ct(2\xi_1 - 1)\Big)}{R}, \quad B_2 = \frac{2\sigma_1(4xR - ct)}{R},\\
A_3 =& 16x^2\sigma_1^6 + 8x\Big(ct + 4x(R-\sigma_1^2)\Big)\sigma_1^4 + 16x(R-\sigma_1^2)\sigma_1^3 + \Big((ct - 4x(R-\sigma_1^2))^2 + 4(R-\sigma_1^2)\Big)\sigma_1^2 -\\
& 4(R-\sigma_1^2)(ct - 4x(R-\sigma_1^2))\sigma_1 + 4(R-\sigma_1^2)^2,\\
A_4 =& 16x^2\sigma_1^6 + 8x\Big(ct + 4x(R-\sigma_1^2)\Big)\sigma_1^4 - 16x(R-\sigma_1^2)\sigma_1^3 + \Big((ct - 4x(R-\sigma_1^2))^2 + 4(R-\sigma_1^2)\Big)\sigma_1^2 +\\
& 4(R-\sigma_1^2)(ct - 4x(R-\sigma_1^2))\sigma_1 + 4(R-\sigma_1^2)^2,\\
A_5 =& 16x^2R^3\sigma_1^2 - 32x^2R^2\sigma_1^4 - 8ctxR^2\sigma_1^2 + 4R^2\sigma_1^2 - 4R^3 + c^2t^2R\sigma_1^2 - 2c^2t^2\sigma_1^4,\\
A_6 =& 2R^2 + \sigma_1^2\Big((ct-4Rx)^2 + 16c\sigma_1^2 tx\Big).
\end{aligned}$$

In Proposition 1, the N-positon obtained from the degenerate Darboux transformation (dDT) combined with higher-order Taylor expansion is a smooth solution. Its structure consists of a mixture of exponential terms and polynomial functions in x and t. This behavior is fundamentally different from that of soliton solutions, which are purely expressed through exponential functions, and rogue waves, which are typically described by rational polynomials. In addition, the correctness of the obtained solutions is guaranteed by the DT framework, which preserves the Lax pair structure. As a result, the transformed solutions automatically satisfy the original equation through the zero-curvature condition.

3.2. *Dynamics of second-order positon solution*

To illustrate the dynamical features, we present the three-dimensional profiles and density distributions of the two-positon solutions q_{2-p} and v_{2-p} in Fig. 1. For a clearer visualization of their propagation paths, the corresponding contour plots are displayed in Figure 1(b) and (e). From Figure 1(c) and (f), it is observed that q_{2-p} and v_{2-p} are not traveling waves with invariant profiles. Instead, their trajectories form slowly varying curves rather than straight lines. Furthermore, the interaction between the two positon components is found to be elastic. The amplitude and overall structure of the second-order positon remain unchanged before and after interaction, apart from a phase shift. In contrast to the classical two-soliton solution, where the phase shift is a constant, the phase shift associated with the second-order positon depends on both x and t.

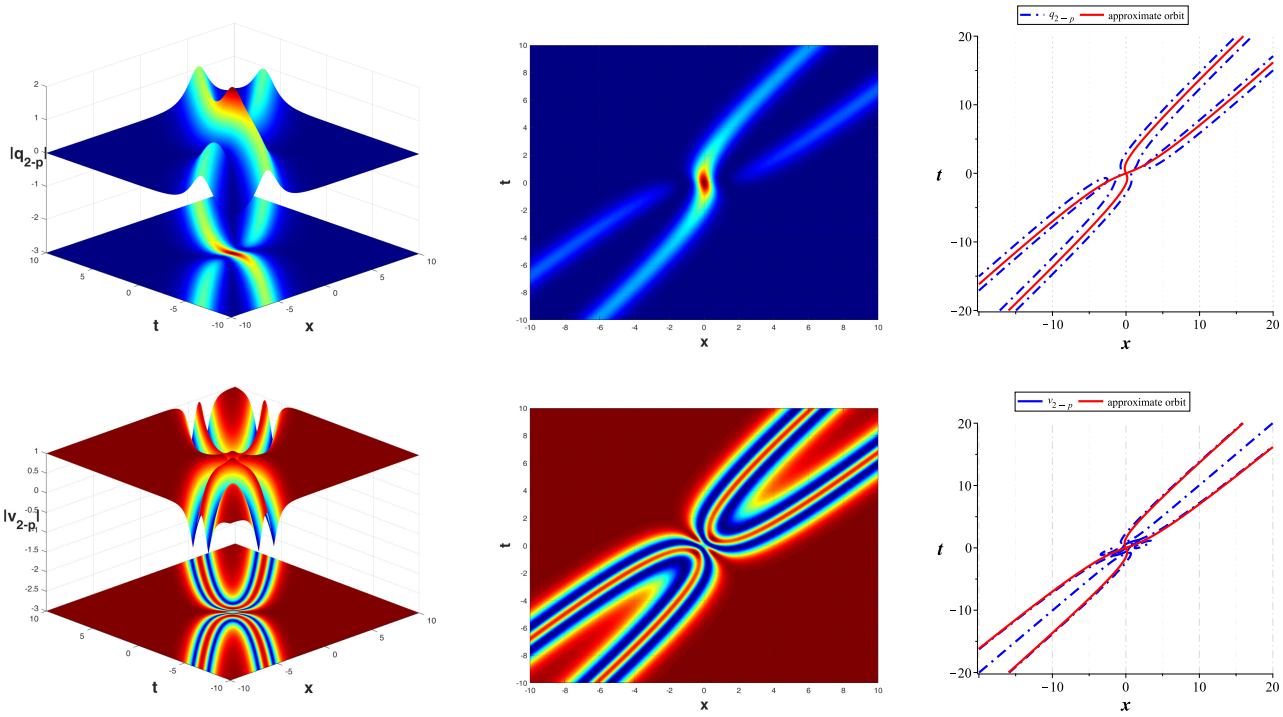

Figure 1. Second-order smooth positon solution of the Kuralay equation with parameters $\xi_1 = 0.5$, $\sigma_1 = 0.6$, and $c = 1$. The first row shows the three-dimensional profile, contour plot, and peak trajectory of $|q_{2-p}|$, together with its peak trajectory. The second row presents the three-dimensional profile of v_{2-p}, its density contour, and the associated dynamical trajectory. These plots illustrate the nontrivial dynamical behavior of the positon solution. In particular, the trajectories of the peaks are not straight lines, indicating that the solution does not propagate as a standard traveling wave. The contour plots further reveal the long-range oscillatory structure and slow decay characteristic of positon solutions.

Since the N-positon solution arises from the degeneration of the N-soliton solution, it remains a nonsingular real solution. To examine the correspondence between positon and soliton dynamics, we compare the approximate peak trajectories of the soliton intensity with those of the positon intensity, as illustrated in Figure 1(c) and (f). It is evident that the two trajectories coincide asymptotically as $|t| \to \infty$. This confirms that the splitting approach provides an accurate description of the positon

dynamics. The same procedure can be extended to higher-order positon solutions. This asymptotic behavior provides a quantitative characterization of the propagation of positon solutions. In particular, the peak trajectories approach well-defined paths as $|t| \to \infty$. In this context, the interaction between positon components can be regarded as elastic, meaning that the amplitude and overall structure of the wave profiles are preserved after interaction. However, unlike classical soliton solutions, the phase shifts of positons are not constant. Due to the presence of polynomial–exponential terms, the phase shift depends on both spatial and temporal variables, leading to more complex dynamical behavior.

From a physical perspective, the non-straight trajectories of the positon peaks indicate that these solutions do not propagate as rigid traveling waves. Instead, their structure evolves dynamically in space and time, reflecting the influence of nonlinear interactions and dispersion. The observed elastic interaction behavior implies that the wave structures preserve their overall amplitude and shape after interaction, which is a characteristic feature of integrable nonlinear systems. However, unlike classical solitons, the phase shifts of positons are not constant, indicating more complex interaction mechanisms.

3.3. Breather-positons of the Kuralay equation

In this subsection, we construct the N-order breather-positon (b-positon) solutions of the Kuralay equation (1.1) under nonvanishing boundary conditions via the dDT. In contrast to the zero seed case, the presence of a nonzero background modifies the spectral structure and leads to oscillatory-type localized patterns.

We begin with the plane-wave seed solution

$$q^{[0]} = Ae^{\mathrm{i}(ax+bt)}, \quad v^{[0]} = b(a-1), \tag{3.7}$$

where A, a, and b are real constants satisfying $b = \frac{a^2}{a-2}$.

Solving the associated spectral problem with this background and choosing $\lambda = \lambda_k$, we obtain the eigenfunctions

$$\psi_1^{(k)} = -\frac{e^{\frac{\mathrm{i}}{2}(ax+bt)}}{2A}\left[(2\mathrm{i}\lambda_k - \mathrm{i}a + \frac{\eta_k}{2})e^{\eta_k x - \frac{b\eta_k t}{(2\lambda_k - 1)}} + (2\mathrm{i}\lambda_k - \mathrm{i}a - \frac{\eta_k}{2})e^{-\eta_k x + \frac{b\eta_k t}{(2\lambda_k - 1)}}\right], \tag{3.8}$$

$$\psi_2^{(k)} = e^{-\frac{\mathrm{i}}{2}(ax+bt)}\left[e^{\eta_k x - \frac{b\eta_k t}{(2\lambda_k - 1)}} + e^{-\eta_k x + \frac{b\eta_k t}{(2\lambda_k - 1)}}\right], \tag{3.9}$$

where

$$\eta_k = \sqrt{-\lambda_k^2 + \lambda_k a - \frac{a^2}{4} - A^2}, \qquad \lambda_k = \xi_k + \mathrm{i}\sigma_k.$$

The complex spectral parameter λ_k determines the oscillatory and localization properties of the solution. When two spectral parameters coalesce, i.e., $\lambda_2 \to \lambda_1 + \epsilon$, and the limit $\epsilon \to 0$ is applied in (3.1), the breather solution degenerates into a second-order b-positon solution.

The resulting solution exhibits periodic modulation along the nonzero background and retains smoothness under the degeneracy limit. Due to the complexity of the explicit expressions, we omit the lengthy formulas and present their dynamical features through graphical illustrations in Figure 2. From a physical perspective, the breather-positon solution represents a modulated nonlinear wave packet evolving on a nonvanishing background. Its oscillatory structure reflects breather-type periodic modulation, while the deformation of the envelope is induced by spectral degeneracy. This hybrid

behavior indicates a more intricate interaction between dispersion, nonlinearity, and background effects than in standard breather solutions.

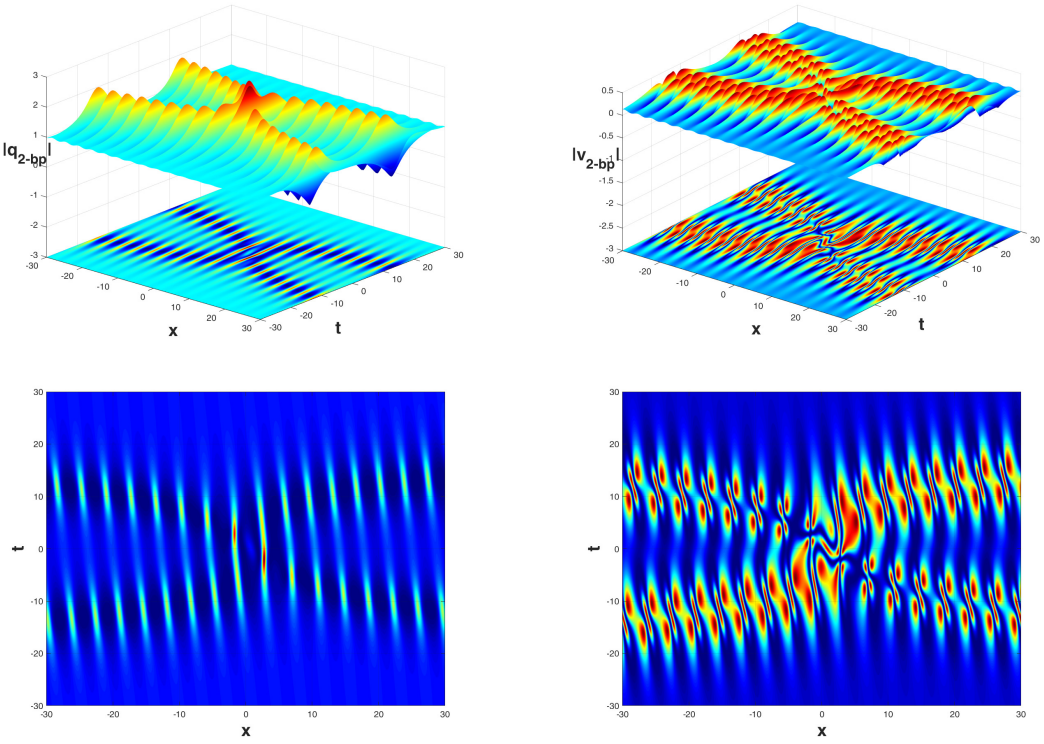

Figure 2. Second-order smooth breather-positon solution of the Kuralay equation. The first row shows the three-dimensional profiles of $|q_{2-bp}|$ and $|v_{2-bp}|$, while the second row presents their corresponding contour plots. Parameters are chosen as $\xi_1 = 0.2$, $\sigma_1 = 0.5$, $A = 1$, with background parameters $(a, b) = \left(\frac{2}{5}, \frac{1}{5}\right)$. These figures demonstrate the hybrid nature of breather-positon solutions. Compared with standard breather solutions, the wave profiles exhibit both oscillatory modulation and algebraic deformation. This reflects the combined effects of spectral degeneracy and nonlinear interaction, leading to more complex spatio-temporal structures.

Classical soliton and breather solutions correspond to distinct spectral parameters in the DT and are typically expressed in terms of exponential functions. These solutions exhibit localized structures with constant phase shifts and well-defined propagation characteristics. In contrast, positon solutions arise from the degeneration of spectral parameters. Their analytical expressions involve a combination of exponential and polynomial terms, which leads to slower spatial decay and long-range oscillatory behavior. In addition, the phase shifts associated with positon interactions are not constant but depend on both space and time. The breather-positon solutions constructed in this work combine the oscillatory features of breathers with the algebraic structure of positons. As a result, they exhibit more complex dynamical behavior compared with standard breather solutions. All figures in this paper were generated using *MATLAB* and *Maple* for numerical evaluation and visualization.

4. Conclusions

In this paper, higher-order smooth positon and breather-positon solutions of the Kuralay equation have been systematically constructed by means of the degenerate Darboux transformation. Starting from the Lax pair formulation, an explicit N-fold DT in determinant form was employed to generate exact solutions of the system. By introducing suitable degeneration procedures for the spectral parameters, higher-order positon solutions were derived from multi-soliton solutions without introducing singularities.

Furthermore, under nonvanishing boundary conditions, higher-order breather-positon solutions were obtained through a similar degeneration mechanism applied to breather solutions. The resulting positon and breather-positon structures exhibit smooth profiles characterized by mixed exponential and polynomial terms, leading to distinct dynamical behaviors compared with classical soliton and breather solutions.

The interaction properties of the obtained solutions were analyzed in detail. It was shown that higher-order positons and breather-positons preserve their structural integrity during propagation and interaction, displaying elastic collision behavior accompanied by nontrivial phase shifts. These features highlight the essential role of spectral degeneracy in shaping the internal dynamics of localized waves in integrable systems.

The results presented in this work enrich the family of exact solutions of the Kuralay equation and provide a unified framework for investigating degenerate localized wave structures in integrable systems. The proposed approach can be extended to other integrable models, offering a useful tool for exploring higher-order positon-type structures and their hybrid generalizations. From a physical viewpoint, the obtained positon and breather-positon solutions represent nonlinear wave structures with long-range interactions and complex dynamical behavior. Their properties, such as non-constant phase shifts and evolving trajectories, distinguish them from classical soliton solutions and provide deeper insight into nonlinear wave propagation in integrable systems.

As exact solutions of an integrable system, the positon and breather-positon solutions constructed in this work are structurally stable within the integrable framework. In particular, their profiles are preserved under the evolution governed by the equation. Nevertheless, a detailed stability analysis under perturbations, such as linear spectral stability or numerical simulations, is beyond the scope of the present study and will be considered in future work.

Author contributions

All authors contributed equally to the preparation of this manuscript. All authors have read and approved the final version of the manuscript for publication.

Use of Generative-AI tools declaration

The authors declare they have not used Artificial Intelligence tools in the creation of this article.

Conflict of interest

All authors declare no conflicts of interest in this paper. Solomon Manukure is a Guest Editor of special issue "Integrable Systems in Higher Dimensions: Geometry, Algebra, and Applications" for AIMS Mathematics. Solomon Manukure was not involved in the editorial review and the decision to publish this article.

References

1. Y. S. Kivshar, B. A. Malomed, Dynamics of solitons in nearly integrable systems, *Rev. Mod. Phys.*, **61** (1989), 763. https://doi.org/10.1103/RevModPhys.61.763
2. M. J. Ablowitz, Z. H. Musslimani, Integrable nonlocal nonlinear Schrödinger equation, *Phys. Rev. Lett.*, **110** (2013), 064105. https://doi.org/10.1103/PhysRevLett.110.064105
3. W. G. Zhang, M. Y. Wang, C. Song, Soliton solutions of the semi-discrete complex coupled dispersionless integrable system, *Appl. Math. Lett.*, **113** (2021), 106859. https://doi.org/10.1016/j.aml.2020.106859
4. H. Ma, R. U. Rahman, S. Manukure, Dynamical analysis and bifurcations in a fractional integrable equation, *Alex. Eng. J.*, **125** (2025), 600–623. https://doi.org/10.1016/j.aej.2025.03.138
5. M. J. Ablowitz, D. J. Kaup, A. C. Newell, H. Segur, The inverse scattering transform-Fourier analysis for nonlinear problems, *Stud. Appl. Math.*, **53** (1974), 249–315. https://doi.org/10.1002/sapm1974534249
6. T. Aktosun, M. Unlu, A generalized method for the Darboux transformation, *J. Math. Phys.*, **63** (2022), 103501. https://doi.org/10.1063/5.0092710
7. W. Yang, C. Wang, Y. Shi, X. Xin, Construction and exact solution of the nonlocal Kuralay-II equation via Darboux transformation, *Appl. Math. Lett.*, **173** (2026), 109758. https://doi.org/10.1016/j.aml.2025.109758
8. R. U. Rahman, Z. Li, J. He, Kink-type wavefronts in some saturated ferromagnetic materials Via the Darboux transformation, *Math. Method. Appl. Sci.*, **48** (2025), 8735–8754. https://doi.org/10.1002/mma.10750
9. K. J. Wang, K. H. Yan, S. Li, Multi-rogue wave, generalized breathers wave, bell shape and singular wave solutions to the (3+1)-dimensional Yu-Toda-Sasa-Fukuyama equation, *Math. Method. Appl. Sci.*, 2026. https://doi.org/10.1002/mma.70663
10. R. Hirota, *The direct method in soliton theory*, Cambridge: Cambridge University Press, 2004. https://doi.org/10.1017/CBO9780511543043
11. L. Huang, D. S. Wang, X. Zhu, Nonlinear Fourier transforms for the Sawada-Kotera equation on the line, *Stud. Appl. Math.*, **155** (2025), e70075. https://doi.org/10.1111/sapm.70075
12. R. U. Rahman, J. He, Degenerate Darboux transformations and the higher-order positon solutions for the principal chiral field equation, *Phys. Lett. A*, **584** (2026), 131634. https://doi.org/10.1016/j.physleta.2026.131634
13. K. J. Wang, K. H. Yan, J. Cheng, Y. B. Zheng, F. Shi, H. W. Zhu, et al., Bilinear form, Bäcklund transformation to the Kairat-II-X-extended equation: N-soliton, anti-kink soliton, novel soliton

molecule, multi-lump and travelling wave solutions, *Mod. Phys. Lett. B*, **40** (2026), 2650057. https://doi.org/10.1142/S0217984926500570

14. K. J. Wang, Exploring exact wave solutions of the Cahn-Allen equation via a novel Bernoulli sub-equation neural networks method, *Mod. Phys. Lett. B*, **40** (2026), 2650062. https://doi.org/10.1142/S0217984926500624
15. P. G. Drazin, R. S. Johnson, *Solitons: An introduction*, Cambridge: Cambridge University Press, 1989. https://doi.org/10.1017/CBO9781139172059
16. J. Yu, F. Yu, Non-autonomous soliton, wave propagation and collision dynamic for (2+1)-dimensional higher-order nonlinear Schrödinger equation with variable coefficients, *Appl. Math. Lett.*, **174** (2026), 109827. https://doi.org/10.1016/j.aml.2025.109827
17. J. J. Huang, Z. L. Jia, X. L. Zhang, Nonlinear interference between solitons and nonstationary dispersive waves in a passively mode-locked fiber laser, *Phys. Rev. A*, **105** (2022), 053526. https://doi.org/10.1103/PhysRevA.105.053526
18. Y. Qi, Q. Yu, Y. Gao, W. Wang, C. Ning, C. He, et al., Dynamics of dissipative pure-quartic solitons and molecules in NPR mode-locked fiber lasers with positive fourth-order dispersion, *Chaos Soliton. Fract.*, **202** (2026), 117579. https://doi.org/10.1016/j.chaos.2025.117579
19. Y. Tao, J. He, Multisolitons, breathers, and rogue waves for the Hirota equation generated by the Darboux transformation, *Phys. Rev. E*, **85** (2012), 026601. https://doi.org/10.1103/PhysRevE.85.026601
20. T. Xu, Y. Wang, Y. Shan, *N*-bright-dark-soliton, the general soliton molecules and *N*-breather for the Kuralay equation, *Phys. Scr.*, **101** (2026), 035207. https://doi.org/10.1088/1402-4896/ae35e7
21. B. Kibler, J. Fatome, C. Finot, G. Millot, F. Dias, G. Genty, et al., The Peregrine soliton in nonlinear fibre optics, *Nature Phys.*, **6** (2010), 790–795. https://doi.org/10.1038/nphys1740
22. L. C. Zhao, L. Ling, Z. Y. Yang, Mechanism of Kuznetsov-Ma breathers, *Phys. Rev. E*, **97** (2018), 022218. https://doi.org/10.1103/PhysRevE.97.022218
23. J. He, H. R. Zhang, L. H. Wang, K. Porsezian, A. S. Fokas, Generating mechanism for higher-order rogue waves, *Phys. Rev. E*, **87** (2013), 052914. https://doi.org/10.1103/PhysRevE.87.052914
24. D. Wang, Z. Liu, H. Zhao, H. Qin, G. Bai, C. Chen, et al., Launching by cavitation, *Science*, **389** (2025), 935–939. https://doi.org/10.1126/science.adu8943
25. Y. H. Jia, Z. Z. Si, Z. T. Ju, H. Y. Feng, J. H. Zhang, X. Yan, et al., Convolutional-recurrent neural network for the prediction of formation and switching dynamics for multicolor solitons, *Sci. China Phys. Mech. Astron.*, **68** (2025), 284211. https://doi.org/10.1007/s11433-025-2679-8
26. V. B. Matveev, Positons: Slowly decreasing analogues of solitons, *Theor. Math. Phys.*, **131** (2002), 483–497. https://doi.org/10.1023/A:1015149618529
27. R. U. Rahman, Z. Li, J. He, Magnetic wave dynamics in ferromagnetic thin films: Interactions of solitons and positons in Landau-Lifshitz-Gilbert equation, *Physica D*, **479** (2025), 134719. https://doi.org/10.1016/j.physd.2025.134719
28. J. Wu, Y. Zhang, X. Wang, J. Wang, Positon and breather positon solutions for the nonlocal higher-order Chen-Lee-Liu equation, *Phys. Lett. A*, **552** (2025), 130630. https://doi.org/10.1016/j.physleta.2025.130630

29. N. V. Priya, S. Monisha, M. Senthilvelan, G. Rangarajan, Nth-order smooth positon and breather-positon solutions of a generalized nonlinear Schrödinger equation, *Eur. Phys. J. Plus*, **137** (2022), 646. https://doi.org/10.1140/epjp/s13360-022-02861-x

30. Y. Zhong, Y. Zhang, Rogue waves on the periodic background of the Kuralay-II equation, *Wave Motion*, **128** (2024), 103310. https://doi.org/10.1016/j.wavemoti.2024.103310

31. Z. Sagidullayeva, G. Nugmanova, R. Myrzakulov, N. Serikbayev, Integrable Kuralay equations: Geometry, solutions and generalizations, *Symmetry*, **14** (2022), 1374. https://doi.org/10.3390/sym14071374

32. Y. Zhong, Y. Zhang, Multi-breather solutions on the periodic background of the Kuralay-II equation, *Phys. Lett. A*, **567** (2025), 131208. https://doi.org/10.1016/j.physleta.2025.131208

33. H. An, Z. Liu, M. Yuen, Novel localized vector wave solutions in the Kuralay-II equation, *Nonlinear Dyn.*, **113** (2025), 23395–23412. https://doi.org/10.1007/s11071-025-11267-0

34. S. O. Abbas, S. Shabbir, S. T. R. Rizvi, A. R. Seadawy, Optical dromions for M-fractional Kuralay equation via complete discrimination system approach along with sensitivity analysis and quasi-periodic behavior, *Mod. Phys. Lett. B*, **39** (2025), 2550048. https://doi.org/10.1142/S0217984925500484

35. A. Hussain, T. F. Ibrahim, M. M. Bashier, W. M. Osman, A. A. Dawood, The profile of soliton molecules for integrable complex coupled Kuralay equations, *Phys. Scr.*, **100** (2025), 015259. https://doi.org/10.1088/1402-4896/ad999d

36. W. A. Faridi, Z. Myrzakulova, R. Myrzakulov, A. Akgül, M. S. Osman, The construction of exact solution and explicit propagating optical soliton waves of Kuralay equation by the new extended direct algebraic and Nucci's reduction techniques, *Int. J. Model. Simulat.*, **45** (2025), 2012–2031. https://doi.org/10.1080/02286203.2024.2315278

37. J. He, L. Zhang, Y. Cheng, Y. Li, Determinant representation of Darboux transformation for the AKNS system, *Sci. China Ser. A*, **49** (2006), 1867–1878. https://doi.org/10.1007/s11425-006-2025-1

AIMS Press